Pattern Recognition Letters 71 (2016) 16–22

Contents lists available at ScienceDirect

Pattern Recognition Letters

journal homepage: www.elsevier.com/locate/patrec

Dominant Rotated Local Binary Patterns (DRLBP) for texture classification☆

Rakesh Mehta*, Karen Egiazarian

Tampere University of Technology, Tampere, Finland

ARTICLE INFO

Article history:
Received 10 April 2015
Available online 30 November 2015

Keywords:
Texture Classification
Local Binary Pattern (LBP)
Rotation Invariance
Feature Selection
Outex
KTH-TIPS

ABSTRACT

In this paper, we present a novel rotation-invariant and computationally efficient texture descriptor called Dominant Rotated Local Binary Pattern (DRLBP). A rotation invariance is achieved by computing the descriptor with respect to a reference in a local neighborhood. A reference is fast to compute maintaining the computational simplicity of the Local Binary Patterns (LBP). The proposed approach not only retains the complete structural information extracted by LBP, but it also captures the complimentary information by utilizing the magnitude information, thereby achieving more discriminative power. For feature selection, we learn a dictionary of the most frequently occurring patterns from the training images, and discard redundant and non-informative features. To evaluate the performance we conduct experiments on three standard texture datasets: Outex12, Outex 10 and KTH-TIPS. The performance is compared with the state-of-the-art rotation invariant texture descriptors and results show that the proposed method is superior to other approaches.

1. Introduction

Texture recognition is an important area of research in computer vision and pattern recognition. It finds numerous applications in industry such as surface inspection, remote sensing, material categorization. Over the years a number of approaches have been proposed for texture classification. Earlier methods were based on filter banks [20], co-occurrence statistics [7] and hidden Markov models [1]. These approaches modeled texture as a 2D surface, therefore, were unable to deal with the viewpoints and 3D transformations. Later, more advanced techniques were applied for texture modeling to achieve robustness to scale, rotation, viewpoints and illumination variations. Among them, the texton based approaches [9,14,23] represent images as histograms of discrete vocabulary of discrete features. They achieve robustness to geometric transformations by capturing the local invariant features. GIST [16] and hierarchical wavelet packet transform (HWVP) [18] describe the coarse structure of images using multi-orientation and multi-resolution Gabor filter banks. These methods consider the perceptual dimensions of images such as roughness, expansion, ruggedness for description. Some recent work based on the compressible nature of texture images [11] and fractal analysis [19] report promising results thanks to a utilization of sparsity.

In the texture classification applications, rotation invariance is often desirable as the material can appear at arbitrary angles because of camera rotation or self-rotation of the captured objects. The rotation invariance approaches in texture classification can be broadly divided into the following three categories: (1) Global image rotation, where the orientation of an image is computed at a holistic level and the image is rotated with respect to it before feature extraction [6,8]; (2) Discard local orientation, where the local features extracted from an image discard any information about the local orientation, e.g., RIFT [9], SRP [11,22]; (3) Local patch rotation, where the local features are extracted by steering the patch along the local dominant direction. The most common example of this category is SIFT [12] which is rotated around the dominant patch orientation. Varma and Zisserman [23] have applied a similar approach to texture classification using filter banks.

The texture descriptor proposed in this paper is based on the Local Binary Pattern (LBP) [15]. LBP has gained a popularity due to its high discriminative power, computational simplicity, invariance to gray scale changes and good performance. In spite of these advantages, application of the traditional LBP is limited since: (1) The descriptor is not invariant to rotations and viewpoints changes; (2) The size of the features increases exponentially with the number of neighbors which leads to an increase of computational complexity in terms of time and space; (3) The structural information captured by it is limited, since only the sign of the pixel difference is used whereas the magnitude information is completely ignored. A number of modifications of LBP have been proposed recently to address the above mentioned limitations. To achieve a rotation invariance, Ojala et al. [15] proposed riLBP

☆ This paper has been recommended for acceptance by Dr. J. Yang.

* Corresponding author. Tel.: +358465423630; fax: +358 3 364 1352.
E-mail address: rakesh.mehta@tut.fi (R. Mehta).

http://dx.doi.org/10.1016/j.patrec.2015.11.019
0167-8655/

descriptors by mapping the rotated variants of the patterns into a rotation invariant prototype. Thus, any information about the local orientation is completely discarded. Zhao et al. [26] observed that the rotation results in the circular shift of the descriptor and proposed LBP-Histogram Fourier (LBP-HF) method by taking the shift invariant Discrete Fourier Transform of the LBP Histogram. The LBP-HF only considers the magnitude spectrum of the transform and the information present in the frequency is ignored. Qian et al. [17] extracted LBP from the image pyramid to capture the multi-resolution information. By using multiple resolutions, various granularities of different scales are captured, however it further increases the dimensionality of the descriptor. Guo et al. [5] proposed Complete LBP by incorporating the sign and the magnitude information in the descriptor. It was demonstrated that the magnitude information can substantially increase the discriminative power of the features. However, due to a sensitivity of the method to illumination changes, the normalization becomes necessary. LBP Variance [6] incorporated the local contrast and the global orientation information into the LBP histogram. However, the above mentioned work achieves a rotation invariance by discarding the local orientation information. Though it results in the invariance, it also leads to a loss of a discriminative information as the local orientation is completely discarded by these approaches. The local patch steering based approaches, which preserves the local orientation information have not been applied for LBP like descriptors.

Another limitation of the original LBP feature is an exponential increase in the number of features with the patch size. With a larger neighborhood a number of patterns do not carry any discriminative information, thus a suitable feature selection mechanism becomes necessary. Ojala et al. [15] were the first to address this issue, proposing the uniform LBP descriptors where the representative subset of patterns is selected corresponding to the frequently occurring patterns (85% total patterns in the Outex dataset). However, for more complex dataset it has been observed that a non-uniform pattern encode the image structure and cannot be ignored. To overcome this problem Liao et al. [10] proposed Dominant LBP, where the training images are used to select the dominating features for each dataset independently. However, they only consider the distribution of the patterns in images while an information about the type of the patterns is completely ignored. Guo et al. [3] proposed Fisher Criterion based features selection, in which dominating patterns are selected from each texture class independently and combined to obtain the final pattern list. By considering the classes independently, the interclass pattern distribution information is discarded, which results in the loss of some discriminative patterns, as will be demonstrated in the experiment section. To overcome the above mentioned shortcomings, in this paper we propose a feature selection method which considers the cumulative distribution of the pattern, thereby selects the features which encode informative structure of images.

The main contributions of the paper are twofold. First, we have observed that the steered local patch approaches are superior to the methods which discard the local orientation. Based on this observation, we propose a patch steered rotation invariance approach. We demonstrate that the commonly used maximum gradient is not suitable for the LBP based descriptor. A novel local orientation estimation approach specifically designed for the LBP type descriptors is proposed. Based on that we design the RLBP descriptor. The preliminary version of the rotation invariance approach has appeared in [13]. In this work we substantiate the earlier findings by providing both theoretical and empirical evidences for our approach. Further, we show that the changes proposed in this work can improve the performance over our earlier work by upto 4–5% in terms of the classification accuracy. The second main contribution is in the feature selection. We address the problem of discriminative pattern selection for the LBP (-like) descriptor in the case of large neighbors. We show empirically that the non-uniform patterns contain discriminative information discarding which results in a loss of information. Then we propose a simple yet powerful feature selection algorithm by considering the cumulative distribution of the patterns in the training samples. Experiments demonstrate that the proposed feature selection approach not only reduces the dimensionality but also increases the discriminative power of the features by discarding the redundant patterns. The code of the algorithm is made publically available [1].

The rest of the paper is organized as follows. In Section 2, we present the proposed approach for texture classification. The results of the experiments are reported in Section 3 and, finally, the paper is concluded in Section 4.

2. Texture classification using DRLBP

In this section we describe in details the proposed approach. First, we provide a background of our approach and give a brief review of LBP. Then we discuss how to achieve a rotation invariance, and finally, we present the algorithm for the features selection.

2.1. Background

Local Binary Patterns operates in a local circular region by taking the difference of the central pixel with respect to its neighbors. It is defined as

$$LBP_{R,P} = \sum_{p=0}^{P-1} s(g_p - g_c) \cdot 2^p,\ \ s(g_p - g_c) = \begin{cases} 1 & g_p \geq g_c \\ 0 & g_p < g_c \end{cases} \tag{1}$$

where g_c and g_p are the gray values of the central pixel and its neighbor, respectively, p is the index of the neighbor, R is the radius of the circular neighborhood and P is the number of the neighbors. If the coordinate of the central pixel is (x, y), then the coordinates of uniformly spaced circular neighborhood are represented as $(x + Rcos(2\pi p/P), y - Rsin(2\pi p/P))$ for $p = 0, 1, 2 \ldots P - 1$. Further the uniform LBP (uLBP), an extension of LBP, considers only the smooth patterns that account for the majority (90%) of the total binary patterns. A local binary pattern is called uniform if the binary code contains at most two transitions from 0 to 1 or vice versa. For example, the patterns 00011100, 01000000 are uniform as both consist of 2 transitions, while 00101000 and 00011010 are non-uniform as these contain 4 transitions.

The LBP operator takes the difference of the central pixel with the neighboring pixels and combines the signs of these differences using unique weights. The order of the weights is fixed in the circular neighborhood, i.e. the weight corresponding to g_0 is always 1, for g_1 it is 2, and so on. If the image undergoes a rotation, the arrangement of the pixels around the center undergoes a shift. Since the order of the weights is fixed, the LBP computed on the rotated images is unable to deal with the rotation changes. Thus, even for a simple image rotation the LBP operator provides very different values. Fig. 1 shows the effect of the rotation on the LBP operator.

It is observed that the performance of the descriptor improves with an increase in the value of P. However, the dimensionality of features also grows exponentially with an increase in the number of neighboring pixels. To reduce this dimensionality, existing methods consider only uniform patterns discarding the rest. Those methods are based on the idea that uniform patterns capture the fundamental structure of texture. We will show that non-uniform patterns also contain an important information ignoring which deteriorates the performance. The reason is that in complex images a non-uniform pattern may also encode the texture structure. Therefore, in our approach we select a subset of the patterns based on their distribution in the training images. It should be noted that the proposed approach significantly differs from DLBP [10] where only the distribution of the patterns in images is considered and information about the type of the patterns is completely ignored.

[1] DRLBP Matlab Code: http://www.cs.tut.fi/~mehta/drlbp .

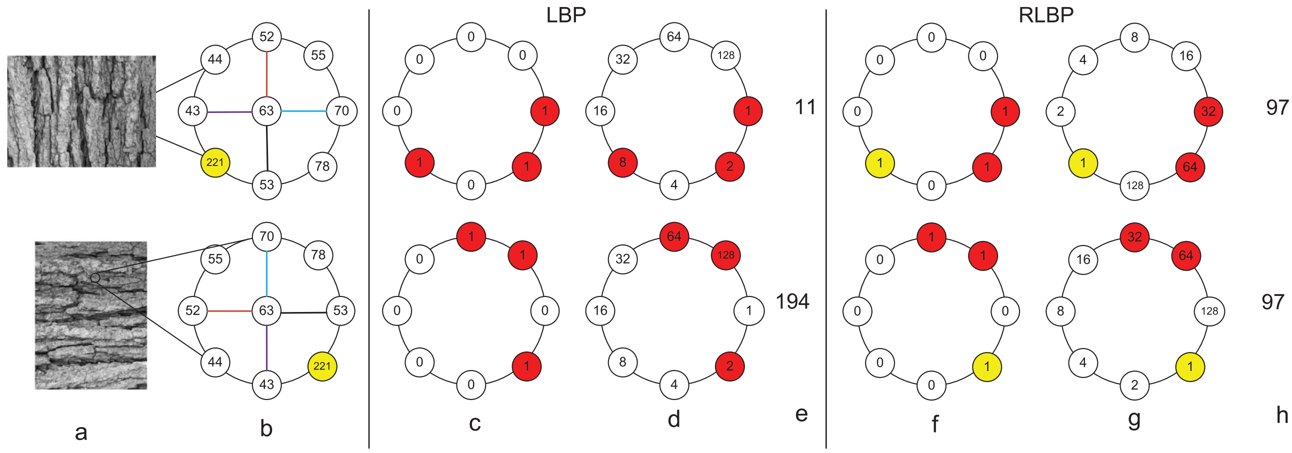

Fig. 1. Effect of rotation on LBP and RLBP operator (a) The image (top) and 90^0 counter-clockwise rotated image (bottom), (b) In the rotated images the neighborhood is rotated counter-clockwise by 90^0, (c) Thresholded neighbors, values above threshold are shown in red color, (d) The weights corresponding to the thresholded neighbors, (e) LBP values, (f) Thresholded neighbors for RLBP with reference denoted in yellow color, (g) The weights of the thresholded neighbors, (h) The RLBP values for the original and rotated image is same. (For interpretation of the references to color in this figure legend, the reader is referred to the web version of this article).

2.2. Rotated Local Binary Pattern

The problem of variations to rotations in LBP arises due to the fixed arrangement of weights. As the weights are aligned in a circular manner, the effect of image rotations can be countered by rotating the weights by the same angle while computing the descriptor. Since the angle of the rotation cannot be known, we propose an adaptive arrangement of weights based on the locally computed reference direction. The reference direction should be such that if an image undergoes a rotation, it should also undergo a rotation by the same angle. In our experiments, we have tested different choices of the reference direction, such as the gradient, weighted difference between the pixels, etc. The best results were obtained with what we call, the *Dominant Direction*. The *Dominant Direction* is defined as the index of the neighboring pixel whose difference from the central pixel is maximum:

$$D = \underset{p\in(0,1...P-1)}{\arg\max} \; |g_p - g_c|. \tag{2}$$

The proposed reference quantizes the dominant directions into P discrete values. The proposed descriptor is computed by rotating the weights with respect to the *Dominant Direction*, hence, the descriptor is called Rotated Local Binary Pattern (RLBP).

Since the dominant direction is taken as the reference in the circular neighborhood, the weights are assigned with respect to it. Thus, the RLBP operator is defined as

$$RLBP_{R,P} = \sum_{p=0}^{P-1} s(g_p - g_c) \cdot 2^{mod(p-D,P)}, \tag{3}$$

where *mod* indicates the modulus operator. In the above definition, the weight term $2^{mod(p-D,P)}$ depends on D. Thus, the *mod* operator circularly shifts the weights with respect to the dominant direction, however, the sequence of the weights remains the same. The shift results in a rotation invariance, as the weights now depend on the neighborhood and not on a pre-selected arrangement. Fig. 1 shows the effect of the rotation on the RLBP features. As before, the red color indicate the pixels above the threshold, yellow color indicate the pixels corresponding to the dominant direction D. The bit corresponding to index D always takes the lowest weight of 1 and other weights are circularly shifted with respect to it. In Fig. 1(g) it can be seen that the weight corresponding to the dominant position is the same both for original and rotated images, although these pixels are at different locations. Thus, the RLBP values obtained for two different rotated neighborhood are similar in this case. It should be mentioned here, for this example the riLBP would also result in the same feature values for rotated and original image, as it maps all the rotated version of a binary pattern to a same feature value. However, if we consider a modified neighborhood where the value 221 is exchanged with the pixel value 78, it corresponds to a different pattern and should be represented by a different feature value. However, the riLBP operator provides the same feature value for this scenario too, as all the rotated patterns result in same value without considering the magnitude of the pixel difference. Thus, the information about the edges is discarded by riLBP, which is taken into account while computing the RLBP feature. The RLBP operator provides a different value for this modified neighborhood, and hence achieves more discriminative power.

A patch rotation using a reference direction is often used to achieve a rotation invariance with the gradient based descriptors such as SIFT. The reference in these descriptors is computed by taking arctan of the X, Y derivative from the image patches. However, the gradient based reference is not suitable for LBP feature as it requires large image patches (usually 16×16) for robust gradient estimation and LBP is often computed on smaller neighborhood. Further, the LBP is a binary descriptor and the dominant gradient reference is not consistent with it. To justify the choice of the proposed reference we compare the proposed *Dominant Direction* with the SIFT based quantized gradient magnitude. For the gradient reference estimation we first compute the gradient of the image, then it is quantized into P partitions and, finally, the descriptor is computed by using the quantized gradient as the reference. Both approaches are evaluated on the Outex dataset and the results are shown in Table 1. The proposed *Dominant Direction* outperforms the gradient based reference in all the scenarios.

Using the proposed *Dominant Direction* as the reference has certain advantages. It is very fast and easy to compute. To compute LBP it is required to evaluate the difference of the neighboring pixels with respect to the central pixel. The same difference is utilized for the computation of *Dominant Direction* therefore there is no increase in the computational complexity over the traditional LBP. Reference index captures the information about the magnitude of the neighboring pixel, which is complementary to the sign. Guo et al. [5] showed

Table 1
Comparison of reference for RLBP.

Datasets	Outex-10	Outex-12
Gradient ref.	96.68	90.15
Dominant Direction	97.34	93.61

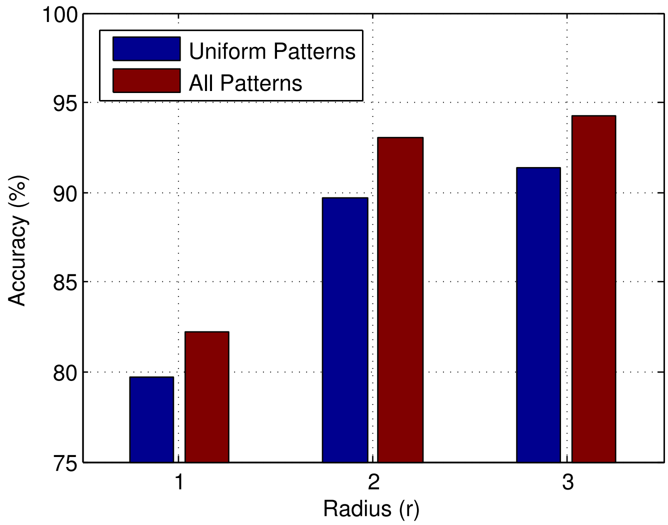

Fig. 2. Classification performance using all patterns and only uniform patterns.

that the magnitude provides a complimentary information that can be used to increase the discriminative power of the operator. Thus, by using the reference direction we also incorporate the complementary information from the local neighborhood based on the magnitude. The information from magnitude is also incorporated in CLBP [5] but it is at the expense of an increase in the dimensionality. However, in the proposed descriptor the dimensionality does not increase.

2.3. Feature selection

In this section we first demonstrate that non-uniform patterns, which are discarded by most of the existing LBP approaches, also contain discriminative information. To analyze the effect of non-uniform patterns we perform the texture classification experiments on Outex-12 dataset. In the first test we perform the classification by considering all the patterns (for $P = 16$, the total number of patterns are 65536). In the second test only the uniform patterns are considered, resulting in a lower dimensional descriptor. The results for the test are shown in Fig. 2. It can be observed that the classification accuracy decreases in the second case, implying that the discriminative information is lost by ignoring the non-uniform patterns. Thus, the idea that uniform patterns are the most discriminative patterns does not generalize across different datasets because for complex images the uniform patterns may not be the most frequently occurring ones.

In this work we propose to learn the subset of discriminative patterns for each dataset from the training images. The most frequently occurring patterns in the training images are selected and are used for classification. If the images have complex structure then the non-uniform patterns may have high occurrence frequency and will be selected. To find the dictionary of the most frequent patterns we apply the following procedure. Let $I_1, I_2 \ldots, I_T$ represent the training images. First, the RLBP histograms $(H_1, H_2, \ldots, H_T)$ are computed for all the training images $(H_i \in \mathbb{R}^{2^P})$. All the histograms are summed together bin-wise to find the patterns distribution from the training images $H = H_1 + H_2 + \cdots + H_T$. The bins of the summed histogram H are sorted in descending order and the patterns corresponding to the first N bins are selected. The value of N is calculated as follows:

$$N = \arg\min_N \frac{\sum_{i=1}^{N-1} H[i]}{\sum_{i=1}^{2^P} H[i]} > \theta. \quad (4)$$

The total number of patterns (N) selected by the algorithm depend on the threshold parameter (θ) and the training data. Hence, the dimensionality of the feature is not constant but varies across different datasets. Fig. 3 shows the proportion of the patterns selected as

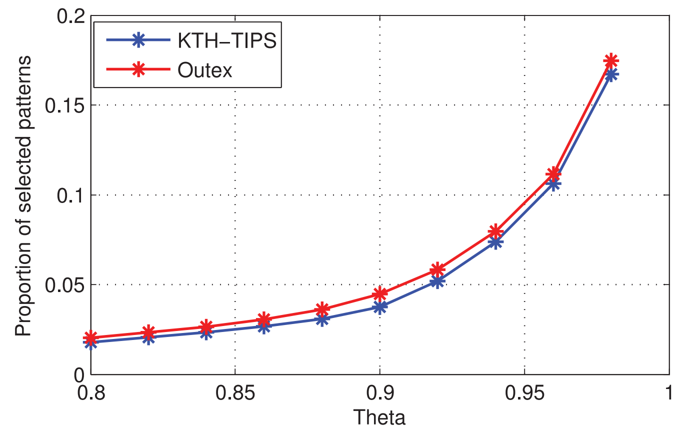

Fig. 3. The proportion of the patterns selected by the proposed feature selection algorithm.

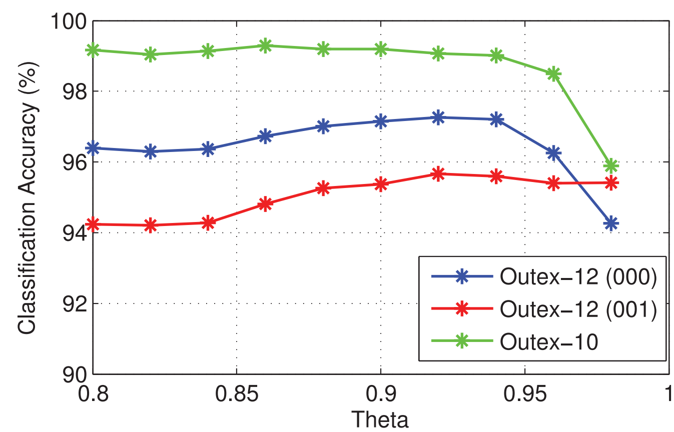

Fig. 4. Classification performance for different datasets saturates around $\theta = 0.9$, with a further increase in the threshold the accuracy drops.

the function of the threshold (θ) for Outex and KTH-TIPS datasets for $P = 16$. Further, the classification accuracy for different test classes of the Outex datasets are shown in Fig. 4. It can be observed that the classification accuracy saturates with the threshold value between 0.85–0.90 in all the datasets. This values results in a significant reduction of the dimensionality as can be observed from Fig. 3. It is also interesting to observe that the accuracy further decreases with an increase in $\theta > 0.95$ values. It is probably due to the selection of the non-discriminative patterns with a larger threshold value. Thus, the proposed approach not only improves the classification accuracy, but it also significantly reduces the dimensionality of the features. The number of selected patterns are between 2–5% of the total number of patterns.

The proposed feature selection approach is simple and easy to implement and has the advantages of both uniform LBP and DLBP. Due to its generality it can be used with any pattern based extensions of LBP for feature selection. Further, an effectiveness of the proposed approach will be demonstrated in the experiments section.

2.4. Classifiers

The classification is performed using Nearest Neighbor (NN) classifier and for a fair comparison with the earlier work on texture classification we use the *Chi Square* kernel. The effectiveness of the *Chi Square* kernel with the pattern based descriptor has been demonstrated by [3,4].

3. Experiments

The proposed method is tested on three different texture datasets: Outex-10, Outex-12, KTH-TIPS and KTH-TIPS-ROT. Outex-10 and Outex-12 have only rotational and illumination variations while the KTH-TIPS dataset also includes scale and viewpoints variations. KTH-TIPS-ROT is an extension of the original KTH-TIPS dataset with rotation variations introduced into it, to analyze the algorithm's robustness to rotation variations. Since a number of descriptors have been developed based on LBP, in our test we first compare the performance with those methods by varying the parameters R and P of the descriptor. The LBP based methods extensively used in this paper are:

LBP: A standard 3x3 neighborhood Local Binary Pattern descriptor. It is denoted in our experiments by LBP and used as a baseline to compare the results on various datasets.

Uniform LBP: The operator considers the patterns with a maximum of two transitions from 0 to 1 and 1 to 0.

Rotation invariant LBP: The rotation invariant modification of LBP proposed in [15]. It rotates the patterns until it will correspond to one of the predefined rotation invariant structure. We denote this descriptor by $riLBP_r$.

LBP-fourier histogram: The rotation invariant LBP which uses DFT to make the pattern invariant to rotation [26]. We denote this descriptor as $LBPHF_r$.

LBP variance: It incorporates local contrast information along with the alignment of the histogram based on a global orientation [6]. In our experiments we represent it as $LBPV_r$.

DRLBP: These are the Dominant Rotated LBP (DRLBP) features proposed in this paper.

uDRLBP: These are the Dominant Rotated LBP (DRLBP) features extracted from the uniform patterns.

It should be noted that the methods LBP and *uLBP* are not rotation invariant and they are used here only as a baseline for comparison. In addition to the above mentioned methods we also compare the performance with other texton based texture descriptors and some other state-of-the-art descriptors proposed recently. Since they do not involve the parameters R and P like in LBP based descriptors, we separately compare their performance on each dataset. The value of θ is set to 0.90 in all our experiments.

3.1. Outex-12

Outex-12 dataset consists of 9120 images from 24 different texture classes under different lighting conditions and rotations. Images from two different classes are shown in Fig. 5(a). We use the standard protocol [6,26] where the testing set consists of $(2 \times 9 \times 20 \times 24) = 8640$ images and training set consists of $(24 \times 20) = 480$ images.

In this experiment we consider both the problems 000 and 001 separately. Unlike most of the work which considers the (R,P) setting as (1,8), (2,16) and (3,24), we test with all possible combinations of R and P. The radius values are chosen as $R = 1, 2, 3$ and number of neighbors as $P = 8, 12, 16$. The maximum value of R is set to 3 because with a larger radius no improvement was observed. The value of P is restricted to 16 because higher values lead to a considerable increase in the dimensionality and computation complexity without any substantial improvement in performance. The results of this experiment are shown in Table 2. It can be observed that the LBP modifications proposed specifically to deal with the rotation changes, such as riLBP, uLBP, LBPHF, LBPV and the proposed descriptor, achieve much better accuracy than the original LBP. Among the earlier LBP versions (LBPri, uLBP), riLBP achieves a relatively high accuracy of 92% and 90% for R = 3 and P = 16. However the dimensionality of the riLBP descriptor for this setting is 4116 which is considerably high. LBPHF performs better than earlier proposed descriptors riLBP and uLBP. Among all these methods the proposed descriptor achieves overall the highest accuracy of 97.15% for $R = 3$ and $P = 12$ for set 000 and the accuracy 95.37% for set 001 with the same parameter setting. Further, it is also interesting to observe that the accuracy of the DRLBP is higher than uDRLBP, which indicates that the non-uniform patterns ignored by the uDRLBP contain certain discriminative information leading to the performance improvement.

Table 2
Test results for Outex-12 dataset.

Test	000			001		
Neighb.	P = 8	P = 12	P = 16	P = 8	P = 12	P = 16
LBP	54.8			56.31		
$uLBP_1$	56.80	57.75	57.52	59.02	59.35	58.70
$uLBP_2$	62.01	60.57	60.60	62.03	60.20	59.86
$uLBP_3$	61.87	62.54	62.82	61.87	60.92	59.51
$riLBP_1$	69.67	74.30	74.30	65.57	70.64	73.28
$riLBP_2$	79.62	86.89	86.34	74.74	83.61	83.93
$riLBP_3$	79.14	88.72	92.84	77.22	86.20	90.92
$LBPHF_1$	70.85	72.63	73.58	77.24	77.50	81.25
$LBPHF_2$	81.20	88.49	87.82	84.21	91.34	92.75
$LBPHF_3$	79.39	89.35	91.08	82.08	90.97	92.40
$LBPV_1$	76.41	84.25	85.55	77.08	82.61	79.97
$LBPV_2$	79.69	86.80	90.25	79.09	84.09	85.67
$LBPV_3$	81.27	87.24	90.85	81.25	85.06	84.76
$uDRLBP_1$	71.73	77.73	78.61	72.98	78.26	78.63
$uDRLBP_2$	83.86	88.96	87.91	81.22	87.22	85.55
$uDRLBP_3$	86.20	90.51	92.03	84.35	88.88	88.81
$DRLBP_1$	73.61	77.19	78.68	75.92	78.44	80.47
$DRLBP_2$	82.19	93.24	90.74	83.70	94.38	90.32
$DRLBP_3$	84.25	92.45	**97.15**	83.19	91.20	**95.37**

In general, it can be observed for all these descriptors, that, the performance increases substantially with the increase in the radii, even when *P* is fixed. In image set 000, when $P = 12$ and *R* is increased from 1 to 3, the increase of the accuracy of uLBP, riLBP, LBPHF and DRLBP is by 5%, 14%, 19% and 15%, respectively. For the same image set when *R* is kept constant and *P* is increased from 8 to 12, the increase in the accuracy is less than the above mentioned values. This is of interest because as the radius is increased the computation complexity and the dimensionality of the descriptor remains the same, thus the performance is improved without any additional computational costs. At the smaller radius the operator captures pixel related information while at the larger radius the region based information is captured. For radius 3 the operator captures the directional information from the circular regions of the diameter 7. Thus, we can say about the texture that it can be more effectively captured from images with the window of size 7×7. As the radius is increased further the accuracy decreases, which is possibly due to the fact that sampling with 12 or 16 pixels values is not sufficient to capture the variations in a patch of size 9×9 or 11×11 pixels.

For better analysis we further give the best results obtained for these methods. Here we present the results as the mean over the

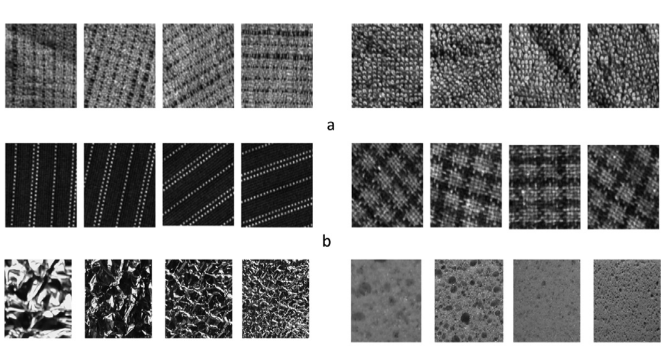

Fig. 5. Examples images from different datasets. For each dataset four images from two different classes are shown. The datasets are (a) Outex-10, (b) Outex-12 and (c) KTH-TIPS.

Table 3
Test results for Outex-10 and KTH-TIPS datasets.

Test	Outex-10			KTH-TIPS		
Neighb.	P = 8	P = 12	P = 16	P = 8	P = 12	P = 16
LBP	50.2			90.97		
$uLBP_1$	57.44	58.35	58.93	85.85	87.07	90.73
$uLBP_2$	59.37	59.63	59.94	87.14	87.92	91.04
$uLBP_3$	59.29	60.39	61.35	90.73	89.26	91.95
$riLBP_1$	82.78	85.85	88.69	83.65	88.29	88.53
$riLBP_2$	83.80	91.48	91.06	84.83	89.75	91.70
$riLBP_3$	80.33	93.30	95.76	85.60	93.17	94.36
$LBPHF_1$	72.03	76.82	83.38	88.73	89.95	89.31
$LBPHF_2$	81.32	90.52	91.77	90.90	90.87	91.41
$LBPHF_3$	84.81	93.51	97.03	89.31	92.09	91.85
$LBPV_1$	91.40	88.93	87.76	78.98	82.96	81.01
$LBPV_2$	92.57	92.18	92.57	78.98	83.0	82.82
$LBPV_3$	92.96	92.13	94.37	79.33	83.58	83.10
$uDRLBP_1$	84.89	86.56	86.95	90.39	90.67	93.12
$uDRLBP_2$	90.57	95.65	94.55	94.53	94.97	94.63
$uDRLBP_3$	91.74	97.24	98.23	93.49	93.04	95.93
$DRLBP_1$	82.23	84.29	84.86	93.17	92.39	92.82
$DRLBP_2$	85.78	96.59	94.47	93.78	94.80	94.32
$DRLBP_3$	88.54	95.94	**99.19**	94.16	**96.78**	90.16

two image sets 000 and 001. We also compare these descriptors with the results reported by other state-of-the-art methods: DLBP [10], *VZ_MR*8 [23], *VZ_Joint* [24], Pyramid LBP [17], Multi Dimensional LBP (MDLBP) [21] and Fisher Based Learning-LBP (FBL-LBP) [3]. The accuracies of these methods are shown in Table 4. For LBP-HF here we report the best accuracy from the original paper [26]. It can be seen that the proposed descriptor achieves the best result, it not only outperforms the binary pattern based approaches but also the texton based methods such as *VZ_MR*8 and *VZ_Joint*. The proposed approach gains $2-3\%$ over the current state-of-the-art, by using just a single scale with parameters $(R=3, P=16)$. FBL-LBP comes second among these descriptors with an accuracy of 92.80%. It should be noted that FBL-LBP achieves this accuracy by the combination of the multiple scales, in their experiment they used the $(8,1)+(16,2)+(24,3)$ to achieve the reported accuracy. The proposed descriptor uses a single scale thus the dimensionality of the descriptor is quite low which makes the classification fast.

3.2. Outex-10

The Outex-10 dataset consists of 4320 images from 24 different textures classes. The images are rotated at nine different angles (0^o, 5^o, 10^o, 15^o, 30^o, 45^o, 60^o, 75^o, 90^o) and the illumination is kept constant. For each angle there are 20 images for each texture class. Examples of images from this dataset are shown in Fig. 5. Following the earlier work [6,26], 20 images corresponding to 0^o, from each class, are used for training and the rest of the images – for testing. Thus, the training set consists of 480 images while the testing set consists of 3840 images. Here we vary the radius as $R=\{1,2,3\}$ and the neighbors parameter as $P=\{8,12,16\}$. The results for different values of R and P are shown in Table 3. Again it can be observed that LBP and uLBP perform poorly as they are not designed to deal with the rotation changes. The rotation invariant approaches perform much better than these baseline methods. The best accuracies achieved by riLBP, LBPHF, LBPV and DRLBP are 97.76, 98.41, 94.37 and 99.19, respectively. The highest accuracy is again achieved by the proposed descriptor DRLBP.

We also compare these descriptors with other state-of-the-art methods: DLBP [10], *VZ_MR*8 filter bank [23], *VZ_Joint* [24], Pyramid LBP [17], Multi Dimensional LBP (MDLBP) [21] and Local Directional Derivative Pattern (LDDP) [4]. In this comparison we have used the best accuracies obtained by the LBP based descriptors compared above. The results for all these descriptors are shown in Table 4. Again it can be observed that the proposed descriptor achieves the highest accuracy among all. A close second is DLBP + NGF which obtains a high accuracy of 99.10.

3.3. KTH-TIPS dataset

The KTH-TIPS database contains 10 texture classes: sandpaper, crumpled aluminium foil, styrofoam, sponge, corduroy, linen, cotton, brown bread, orange peel and cracker. Images were captured at nine different scales, covering two octaves, under three different poses and three illumination conditions. Thus, there are a total of 9 images per scale, and 81 images per material. In this experiment we follow the protocol of LBPV [6], where 40 images from each class are used as training data and the rest of the images are used for testing. The dataset is different from the previous Outex dataset in the sense that it also contains the scale variations in the images. Therefore the protocol followed for testing this dataset considers much more training images compared to Outex dataset, which helps in learning and dealing with the scale changes.

The experiments are repeated 10 times with randomly chosen training samples and the mean accuracies are reported. The results for the LBP based descriptors for different radius (R=1,2,3) and neighbors $P=8,12,16$ are shown in Table 3. It can be observed that the proposed descriptor outperforms all the other descriptors for all different parameter values. Even with a small number of neighbors $P=8$ it achieves a high accuracy of 94.29%. The best results are obtained for $P=12$ and $R=3$ with the DRLBP descriptor. It gains by 5% over LBP-HF which achieves the highest accuracy of 92.09%. Again, it can be observed that the DRLBP achieves better accuracy than uDRLBP suggesting that the proposed feature selection algorithm which considers the non-uniform patterns helps in improving the performance.

Again we compare the performance of these descriptors with the other state-of-the-art descriptors in Table 4. Here we use the descriptors: *VZ_MR*8, *VZ_Joint*, Local Energy Patterns [25], and BIF [2] for the comparison of results. Among all these descriptors, the BIF method achieves the best result, however the proposed approach is comparable to it.

3.4. KTH-TIPS-ROT dataset

The images of original KTH-TIPS dataset do not have any rotation variance. In order to test the algorithms for rotation variation we modify the original dataset by introducing rotation variations in the original images. Each image in the dataset is randomly rotated by an angle between $0-360^o$ and 100×100 cropped images around the center of the rotated image are extracted. In the experiment we use the same evaluation protocol as the original KTH-TIPS dataset, where

Table 4
Comparison with other methods.

Method	*LBP*	*uLBP*	*riLBP*	*LBPHF*	*LBPV*	*DLBP + NGF*	*VZ_MR8*	*VZ_J*	*PLBP*	*MDLBP*	*FBLLBP*	*BIF*	*MLEP*	*Proposed*
Outex-12	54.80	64.30	91.50	94.90	87.96	91.80	92.68	91.72	87.79	91.96	92.80	–	–	**96.26**
Outex-10	54.80	61.35	95.76	98.04	94.37	99.10	93.59	92.00	96.64	95.34	98.64	–	–	**99.19**
KTH-TPS	93.95	94.85	94.87	91.73	87.96	–	93.50	95.46	–	–	–	**98.50**	96.41	96.78
KTH-TPS-ROT	65.45	66.34	83.49	83.57	77.73	–	–	–	–	–	–	–	–	**89.46**

40 randomly selected images in each class are used for training and the rest are used for testing.

The performance of the proposed approach is compared with the LBP based descriptors LBP, uLBP, riLBP, LBP-HF and LBPV. Best performances achieved by these descriptor are reported in Table 4. It can be observed that the best classification accuracy is achieved by the proposed approach. As expected the performance of all the descriptors drops for this datasets, as the rotation variations make the classification more difficult. However, the proposed descriptor still outperforms other LBP extensions such as LBP-HF, LBPV by a margin indicating its robustness to the rotation variations.

4. Conclusions

In this paper we have proposed a so-called Dominant Rotated Local Binary Pattern (DRLBP) descriptor for texture classification. We specifically addressed the problems of rotation invariance and feature selection. Rotation invariance is achieved by computing the descriptor with respect to a local reference. Dominant direction is proposed as a local reference that is easy to compute and invariant to monotonic gray scale variations. Feature selection is based on the dominant patterns learned from the training data. Extensive experiments have been conducted on three standard texture datasets that include rotation and also scale variations. The obtained results demonstrate that the proposed descriptor outperforms not only a number of LBP based descriptors but also other state-of-the-art approaches for texture classification.

References

[1] J.-L. Chen, A. Kundu, Rotation and gray scale transform invariant texture identification using wavelet decomposition and hidden Markov model, IEEE Trans. Pattern Anal. Mach. Intell. 16 (2) (1994) 208–214.
[2] M. Crosier, L.D. Griffin, Using basic image features for texture classification, Int. J. Comput. Vis. 88 (3) (2010) 447–460.
[3] Y. Guo, G. Zhao, M. Pietikäinen, Z. Xu, Descriptor learning based on fisher separation criterion for texture classification, Proceedings of Asian Conference on Computer Vision (ACCV) (2010) 185–198.
[4] Z. Guo, Q. Li, J. You, D. Zhang, W. Liu, Local directional derivative pattern for rotation invariant texture classification, Neural Comput. Appl. 21 (8) (2012) 1893–1904.
[5] Z. Guo, L. Zhang, D. Zhang, A completed modeling of local binary pattern operator for texture classification, IEEE Trans. Image Process. 19 (6) (2010) 1657–1663.
[6] Z. Guo, L. Zhang, D. Zhang, Rotation invariant texture classification using LBP variance (LBVP) with global matching, Patt. Recognit. 43 (3) (2010) 706–719.
[7] R. Haralick, Statistical and structural approaches to texture, Proc. IEEE 67 (5) (1979) 786–804.
[8] K. Jafari, H. Soltanian, Radon transform orientation estimation for rotation invariant texture analysis, IEEE Trans. Pattern Anal. Mach. Intell. 27 (6) (2005) 1004–1008.
[9] S. Lazebnik, C. Schmid, J. Ponce, A sparse texture representation using local affine regions, IEEE Trans. Pattern Anal. Mach. Intell. 27 (8) (2005) 1265–1278.
[10] S. Liao, W. Law, A.C. Chung, Dominant local binary patterns for texture classification, IEEE Trans. Image Process. 18 (5) (2009) 1107–1118.
[11] L. Liu, P. Fieguth, D. Clausi, G. Kuang, Sorted random projections for robust rotation-invariant texture classification, Pattern Recognit. 45 (6) (2012) 2405–2418.
[12] D.G. Lowe, Distinctive image features from scale-invariant keypoints, Int. J. Comput. Vis. 60 (2) (2004) 91–110.
[13] R. Mehta, K. Egiazarian, Rotated local binary pattern (RLBP) rotation invariant texture descriptor, Proceedings of International Conference on Pattern Recognition Applications and Methods (2013) 497–502.
[14] R. Mehta, K. Egiazarian, Texture classification using dense micro-block difference (DMD), Asian Conf. Comput. Vis. (ACCV) (2014).
[15] T. Ojala, M. Pietikainen, T. Maenpaa, Multiresolution gray-scale and rotation invariant texture classification with local binary patterns, IEEE Trans. Pattern Anal. Mach. Intell. 24 (7) (2002) 971–987.
[16] A. Oliva, A. Torralba, Modeling the shape of the scene: a holistic representation of the spatial envelope, Int. J. Comput. Vis. 42 (3) (2001) 145–175.
[17] X. Qian, X.-S. Hua, P. Chen, L. Ke, Plbp: an effective local binary patterns texture descriptor with pyramid representation, Patt. Recognit. 44 (10) (2011) 2502–2515.
[18] X. Qian, G. Liu, D. Guo, Z. Li, Z. Wang, H. Wang, Object categorization using hierarchical wavelet packet texture descriptors, in: Proceedings of IEEE International Symposium on Multimedia, IEEE, 2009, pp. 44–51.
[19] Y. Quan, Y. Xu, Y. Sun, Y. Luo, Lacunarity analysis on image patterns for texture classification, in: Proceedings of IEEE Conference on Computer Vision and Pattern Recognition, IEEE, 2014, pp. 160–167.
[20] T. Randen, J. Husoy, Filtering for texture classification: a comparative study, IEEE Trans. PAMI 21 (4) (1999) 291–310.
[21] G. Schaefer, N.P. Doshi, Multi-dimensional local binary pattern descriptors for improved texture analysis, in: Proceedings of International Conference on Pattern Recognition, 2012, pp. 2500–2503.
[22] H. Skibbe, M. Reisert, T. Schmidt, T. Brox, O. Ronneberger, H. Burkhardt, Fast rotation invariant 3d feature computation utilizing efficient local neighborhood operators, IEEE Trans. Pattern Anal. Mach. Intell. 34 (8) (2012) 1563–1575.
[23] M. Varma, A. Zisserman, A statistical approach to texture classification from single images, Int. J. Comput. Vis. 62 (1-2) (2005) 61–81.
[24] M. Varma, A. Zisserman, A statistical approach to material classification using image patch exemplars, IEEE Trans. Pattern Anal. Mach. Intell. 31 (11) (2009) 2032–2047.
[25] J. Zhang, J. Liang, H. Zhao, Local energy pattern for texture classification using self-adaptive quantization thresholds, IEEE Trans. Image Process. 22 (1) (2013) 31–42.
[26] G. Zhao, T. Ahonen, J. Matas, M. Pietikainen, Rotation-invariant image and video description with local binary pattern features, IEEE Trans. Image Process. 21 (4) (2012) 1465–1477.